

Synthesis and Properties of Highly Fluorescent
Indolizino[3,4,5-*ab*]isoindolesTeruyuki Mitsumori,[†] Michael Bendikov,[†] Olivier Dautel,[†] Fred Wudl,^{*,†}
Takeshi Shioya,[‡] Hideki Sato,[‡] and Yoshiharu Sato[‡]*Contribution from the Department of Chemistry and Biochemistry, Exotic Materials Institute,
University of California, Los Angeles, California 90095-1569, and Science & Technology
Research Center, Mitsubishi Chemical Corporation, 1000 Kamoshida Aoba,
Yokohama 227, Japan*

Received February 12, 2004; E-mail: wudl@chem.ucla.edu

Abstract: We report here the synthesis, X-ray structures, optical and electrochemical properties, fabrication of light-emitting devices, and density functional calculations for indolizino[3,4,5-*ab*]isoindole (**INI**) derivatives. Strongly luminescent heterocycles based on the **INI** unit were synthesized by 1,3-dipolar cycloaddition reactions between pyrido[2,1-*a*]isoindole (**PIS**) and acetylene or ethylene derivatives. They are indolizino[3,4,5-*ab*]isoindoles **2–9** and **14–15**, benzo[1',2'-1,2]indolizino[3,4,5-*ab*]isoindoles **10**, pyridazino[4',5':1,2]-indolizino[3,4,5-*ab*]isoindoles **12–13**, and 2,3-hydropyridazino[4',5':1,2]indolizino[3,4,5-*ab*]isoindole-1,4-dione **11**. The relative luminescence quantum yield can be as high as 90%. Their reduction and oxidation potentials and high luminescence can make these heterocycles possible alternatives to tris(8-hydroxyquinolinato)aluminum (Alq₃). The brightness of the light-emitting device reached as high as 10⁴ cd/m² and indolizino[3,4,5-*ab*]isoindole **3** emits beautifully blue light. The X-ray crystal structures of **INI** derivatives were obtained for the first time. The geometries obtained from X-ray data and density functional theory calculations shed more light on an interesting formally antiaromatic 16 π system, which is divided into 10 π and 6 π aromatic systems. We also report a relatively easy protonation of **INI**, which occurs at a carbon, rather than nitrogen atom.

Introduction

Light-emitting organic compounds (organic luminophors) continue to arouse strong interests because of their fascinating functions as electroluminescent materials, sensors, lasers, and other semiconductor devices.¹ Among these applications, organic light-emitting diodes (OLEDs) have been most widely investigated.² Two types of organic materials, small molecules and polymers, are commonly used for OLEDs. Small molecules have the advantages of facile emission color control and ease of fabrication of multilayer devices. They, however, still have

stability problems, and rules governing the correlation between structure and fluorescence efficiency are still in their infancy.³

While many chromophores have been designed and synthesized for potential OLEDs,^{4,5} it is essential to find molecules which exhibit high fluorescence, little self-quenching, ideal HOMO and LUMO energy levels, pure red-green-blue (RGB) color, and high stability. Among the chromophores, tris(8-hydroxyquinolinato)aluminum (Alq₃) is most commonly used and known to be a good emitting and an electron transport material. However, its electron mobility (on the order of 10^{−5} cm²/V·s)⁶ and hydrolytic stability could be improved; also its ligands have been suspected to be toxic.⁷

Recently our group has reported a series of highly blue fluorescent pyrrolopyridazines, which are expected to be good

[†] University of California, Los Angeles.[‡] Mitsubishi Chemical Corp.

- (1) (a) Tullo, A. H. *Chem. Eng. News* **2000**, 78, 25. (b) Tang, C. W.; Van Slyke, S. A. *Appl. Phys. Lett.* **1987**, 51, 913. (c) Woo, H. S.; Czerw, R.; Webster, S.; Carroll, D. L.; Ballato, J.; Strevens, A. E.; O'Brien, D.; Blau, W. J. *Appl. Phys. Lett.* **2000**, 77, 1393. (d) Chen, L.; McBranch, D. W.; Wang, H.-L.; Helgeson, R.; Wudl, F.; Whitten, D. C. *Proc. Natl. Acad. Sci. U.S.A.* **1999**, 96, 12287. (e) Hide, F.; Díaz-García, M. A.; Schwartz, B. J.; Andersson, M.; Pei, Q.; Heeger, A. J. *Science* **1996**, 273, 1833. (f) Swager, T. M. *Acc. Chem. Res.* **1998**, 31, 201. (g) Pei, Q.; Yu, G.; Zhang, C.; Yang, Y.; Heeger, A. J. *Science* **1995**, 269, 1086.
- (2) (a) Tang, C. W.; VanSlyke, S. A.; Chen, C. H. *J. Appl. Phys.* **1989**, 3610. (b) Burroughes, J. H.; Bradley, D. D. C.; Brown, A. R.; Marks, R. N.; Mackay, K.; Friend, R. H.; Burns, P. L.; Holmes, A. B. *Nature* **1990**, 347, 539. (c) Braun, D.; Heeger, A. J. *Appl. Phys. Lett.* **1991**, 58, 1982. (d) Kepler, R. G.; Beeson, P. M.; Jacobs, S. J.; Anderson, R. A.; Sinclair, M. B.; Valencia, V. S.; Cahill, P. A. *Appl. Phys. Lett.* **1995**, 66, 3618. (e) Thompson, M. A.; Forrest, S. R. *Nature* **2000**, 403, 750. (f) Srdanov, G.; Wudl, F. U.S. Pat. No. 5,189,136, 1993. (g) Lee, S. H.; Nakamura, T.; Tsutsui, T. *Org. Lett.* **2001**, 3, 2006. (h) Noda, T.; Shirota, Y. *J. Am. Chem. Soc.* **1998**, 120, 971. (i) Sheats, J. R.; Antoniadis, H.; Hueschen, M.; Leonard, W.; Miller, J.; Moon, R.; Roitman, D.; Stocking, A. *Science* **1996**, 273, 884. (j) Goldfinger, M. B.; Crawford, K. B.; Swager, T. M. *J. Am. Chem. Soc.* **1997**, 119, 4578. (k) Neef, C. J.; Ferraris, J. P. *Macromolecules* **2000**, 33, 2311. (l) Pei, Q.; Yang, Y. *J. Am. Chem. Soc.* **1996**, 118, 7416. (m) Ego, C.; Marsitzky, D.; Becker, S.; Zhang, J.; Grimdale, A. C.; Müllen, K.; MacKenzie, J. D.; Silva, C.; Friend, R. H.; *J. Am. Chem. Soc.* **2003**, 125, 437.
- (3) (a) Willardson, R. K.; Weber, E.; Mueller, G.; Sato, Y. *Electroluminescence I, Semiconductors and Semimetals Series*; Academic Press: New York, 1999. (b) Bulovic, V.; Forrest, S. R.; Mueller-Mach, R.; Mueller, G. O.; Leslele, M.; Li, W.; Ritala, M.; Neyts, K. *Electroluminescence II, Semiconductors and Semimetals Series*; Academic Press: New York, 2000.
- (4) Chen, C. H.; Shi, J. *Coord. Chem. Rev.* **1998**, 171, 161.
- (5) Kido, J.; Okamoto, Y. *Chem. Rev.* **2002**, 102, 2357.
- (6) (a) Barth, S.; Muller, P.; Riel, H.; Seidler, P. F.; Riess, W.; Vestweber, H.; Bassler, H. *J. Appl. Phys.* **2001**, 89, 3711. (b) Brütting, W.; Berleb, S.; Muckl, A. *G. Synth. Met.* **2001**, 122, 99.
- (7) Bernstein, E. H.; Pienta, P. W.; Gershon, H. *Toxicol. Appl. Pharmacol.* **1963**, 33, 599.

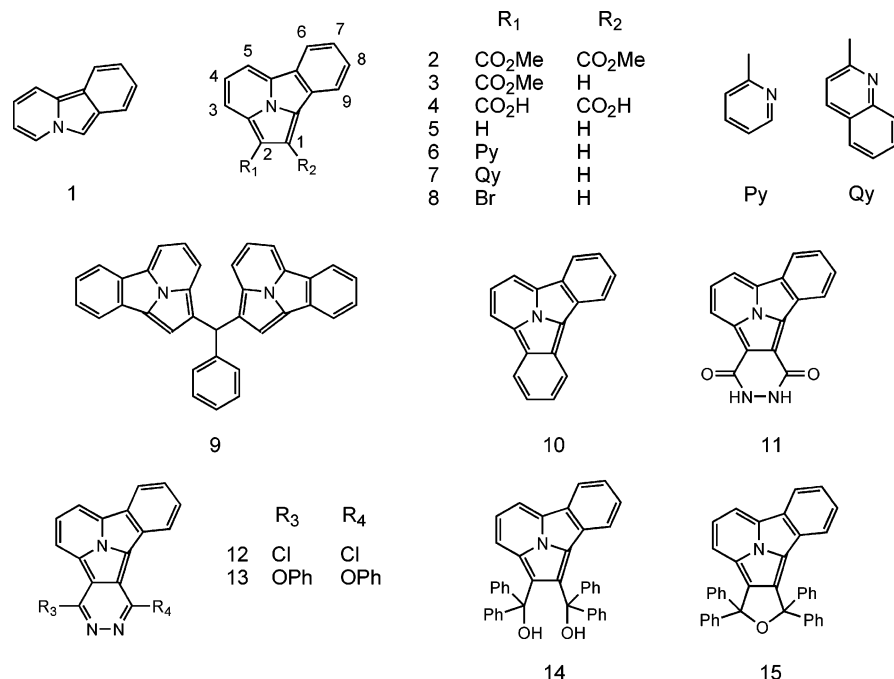


Figure 1. Synthesized heterocyclic molecules used in this paper.

chromophores for highly efficient OLEDs.⁸ During our studies, we found a series of indolizino[3,4,5-*ab*]isoindole (**INI**) with quite interesting luminescence characteristics. Herein we report the synthesis and the properties of 14 **INIs**⁹ which were synthesized from pyrido[2,1-*a*]isoindole (**PIS**). This is the first paper where the excellent luminescence and excellent LED device performance, X-ray crystal structures, protonation, and electronic properties of **INIs**, as well as theoretical studies and applicability of **INIs** as an active semiconductor in field effect transistors are reported. These heterocycles have excellent luminescence (quantum efficiencies are as high as 90%) and different emission colors (from blue to green), and their HOMO and LUMO levels are easily tunable to afford compounds for device fabrication. The structural data, combined with density functional calculations, allowed for a better understanding of the **INI** chromophore.

Results and Discussion

Synthesis. Compounds reported in this paper are presented in Figure 1. Synthetic strategies for the **INIs** are depicted in Scheme 1.

As shown in Scheme 1, the preparation of **INIs** were initially carried out by cycloaddition with **PIS** (**1**), which was prepared

according to a modified literature procedure¹⁰ and used freshly due to its sensitivity to oxygen.¹¹ Cycloadditions occurred smoothly when acetylene or ethylene derivatives were added. For compounds **6** and **7**, vinyl pyridine and vinylquinoline were not reactive enough so that acetylene derivatives were used. Oxidative dehydrogenations were performed using chloranil and sulfur (except compound **10**,^{9f} which had been oxidized by air). Adducts **6a** and **7a** are relatively stable toward oxidation, so they needed stronger condition for aromatization (sulfur, around 130 °C).

Starting from compound **2** nine heterocycles were synthesized. They are indolizino-isoindoles (**4**, **5**, **8**, **9**, **14**), furan-fused heterocycles (**15**), and pyridazine-fused heterocycles (**11**–**13**). First, compound **2** was hydrolyzed quantitatively to obtain compound **4** that was consequently decarboxylated by copper chromite at high temperature (210 °C).^{9c} The resulting heterocycle **5** is unusually nucleophilic toward electrophilic substitution. From the results of NMR, mass spectra, and calculations (see below), the substitution is expected to occur at position 2. Compound **5** was easily brominated at moderately low temperature (0 °C) without any catalyst to afford bromide **8** and was also easily dimerized with benzaldehyde with a catalytic amount of acid to form compound **9**. Compound **2** was allowed to react with phenyllithium to obtain a tetraphenyl adduct **14**, which subsequently, upon acid treatment, formed **15**. Treatment of **2** with hydrazine¹² formed hydrazide **11**, whose fused ring was subsequently aromatized with PCl₅ to form pyridazine-fused heterocycle **12**. The chlorides in **12** were easily displaced by phenoxide¹³ to afford **13** in good yield.

For benzannulated compound **10**, benzyne was used as an acetylene derivative. Compound **1** was allowed to react with

(8) (a) Cheng, Y.; Ma, B.; Wudl, F. *J. Mater. Chem.* **1999**, *9*, 2183. (b) Mitsumori, T.; Bendikov, M.; Sedó, J.; Wudl, F. *Chem. Mater.* **2003**, *15*, 3759.

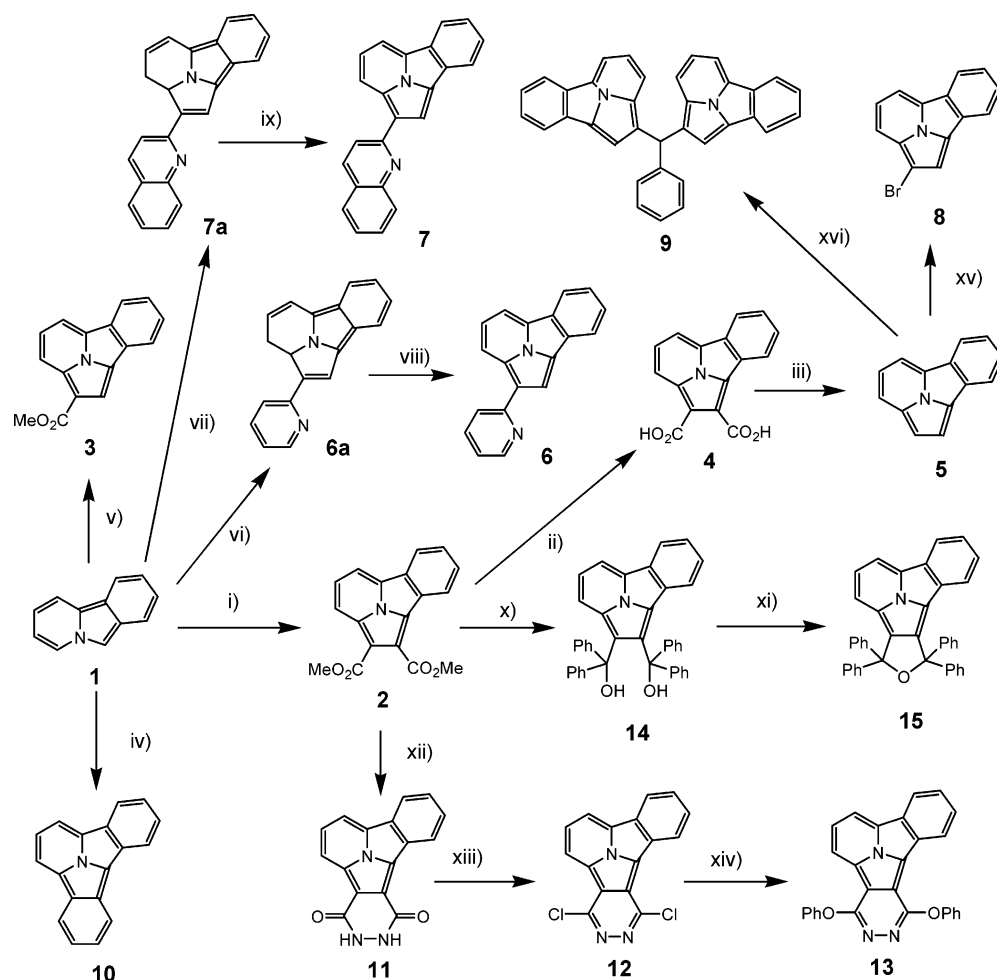
(9) Synthesis and properties of some **INIs** (**2**,^{a-c} **3**,^{a,b} **4**,^c **5**,^{b-e} **10** f–k) have been previously reported. (a) Kajigaesh, S.; Mori, S.; Fujisaki, S.; Kanemasa, S. *Bull. Chem. Soc. Jpn.* **1985**, *58*, 3547. (b) Matsumoto, K.; Uchida, T.; Kato, T.; Toda, M.; Aoyama, K.; Konishi, H. *Heterocycles* **1990**, *31*, 593. (c) Tominaga, Y.; Shiroshita, Y.; Gotou, H.; Matsuda, Y. *Heterocycles* **1986**, *24*, 3071. (d) Castle, L. W.; Tominaga, Y.; Castle, R. N. *J. Heterocycl. Chem.* **1995**, *32*, 1033. (e) Tominaga, Y.; Shigematsu, Y.; Saeki, K. *J. Heterocycl. Chem.* **2002**, *39*, 571. (f) Yamauchi, J.; Uchida, T.; Matsumoto, K. *Heterocycles* **1990**, *31*, 1785. (g) Matsumoto, K.; Yamauchi, J.; Uchida, T. *Heterocycles* **1985**, *23*, 2773. (h) Uchida, T.; Aoyama, K.; Nishikawa, M.; Kuroda, T.; Okamoto, T. *J. Heterocycl. Chem.* **1988**, *25*, 1793. (i) Matsumoto, K.; Uchida, T.; Sugi, T.; Yagi, Y. *Chem. Lett.* **1982**, 869. (j) Matsumoto, K.; Katsura, H.; Uchida, T.; Aoyama, K.; Machiguchi, T. *J. Chem. Soc., Perkin Trans. 1* **1996**, *21*, 2599. (k) Matsumoto, K.; Katsura, H.; Yamauchi, J.; Uchida, T.; Aoyama, K.; Machiguchi, T. *Bull. Soc. Chim. Fr.* **1996**, *133*, 891.

(10) Fozard, A.; Bradsher, C. K. *J. Org. Chem.* **1967**, *32*, 2966.

(11) Bradsher, C. K.; Voigt, C. F. *J. Org. Chem.* **1971**, *36*, 1603.

(12) Clifford, M. C. *Synth. Commun.* **1989**, *19*, 1981.

(13) Becker, H.; King, S. B.; Taniguchi, M.; Vanhessche, K.; Sharpless, K. B. *J. Org. Chem.* **1995**, *60*, 3940.

Scheme 1. Synthetic Route to 2–15^a

^a (i) Dimethyl maleate, CH₂Cl₂, 0 °C, 1 h; (ii) NaOH(aq), THF, reflux, 5 h; (iii) 2CuO·Cr₂O₃, quinoline, 210 °C, 4 h; (iv) 2,2,6,6-tetramethylpiperidine, *n*-BuLi, bromobenzene, THF, −78 °C, 1 h; (v) methyl acrylate, CH₂Cl₂, 0 °C, 1 h; (vi) 2-ethynylpyridine, dichloroethane, 0 °C, 1 h; (vii) 2-ethynylquinoline, dichloroethane, 0 °C, 1 h; (viii) sulfur, chlorobenzene, reflux, 10 h; (ix) sulfur, chlorobenzene, reflux, 10 h; (x) phenyllithium, THF, −75 °C, 4 h; (xi) acetic acid, THF, 80 °C, 4 h; (xii) hydrazine, EtOH, chlorobenzene, reflux, 5 days; (xiii) PCl₅, POCl₃, 130 °C, 4 h; (xiv) phenol, K₂CO₃, DMF, reflux, 3 days; (xv) bromine, CH₂Cl₂, −10 °C, 1 h; (xvi) benzaldehyde, *p*-toluenesulfonic acid, THF, 50 °C, 3 h.

benzynes, which were generated from bromobenzene, to afford compound **10**.

Optical Properties. The absorption and fluorescence spectra were recorded in dimethyl sulfoxide (DMSO), methanol, methylene chloride, tetrahydrofuran (THF), hexane, and acetic acid at room temperature.^{14,15} As shown in Table 1 and Figure 2, the INIs are highly luminescent and emit light from blue to green.¹⁶ While the quantum efficiencies (QE) are solvent-dependent, most compounds reach efficiencies of 80–90%, except **7** and **10**. The brominated compound **7** has lower QE, probably due to heavy atom effect.¹⁷ Interestingly most Stokes shifts were quite small (except that of compound **2**),¹⁸ less than 20 nm and even less than 10 nm in a nonpolar solvent, such as hexane. Apparently the INIs are so rigid that there is very little

Table 1. Quantum Efficiency (%) of Compounds 2–15 in Different Solvents

	MeOH	CH ₂ Cl ₂	DMSO	hexane	THF	AcOH
2	82	68	71	55	69	81
3	80	57	79	68	69	88
4	78	40	62	-	71	78
5	55	45	79	32	46	79
6	77	74	87	63	80	3
7	92	81	78	89	87	<0.1
8	9	9	8	7	8	8
9	74	83	79	34	64	58
10	29	26	40	18	31	33
11	26	-	25	-	37	82
12	47	45	44	-	51	19
13	78	67	82	53	74	62
14	58	62	74	42	82	83
15	51	63	76	-	64	88

(14) Sharma, A.; Schulman, S. G. *Fluorescence Spectroscopy*; John Wiley & Sons: New York, 1999.

(15) Relative quantum yields were determined by using perylene in degassed cyclohexane ($\Phi = 0.94$) as reference; see: Berlman, I. *Handbook of Fluorescence Spectra of Aromatic Molecules*; Academic Press: New York, 1965.

(16) Absorption and fluorescence spectra of all INIs synthesized as well as λ_{max} of the absorption spectra, λ_{max} of the fluorescence spectra, and the Stokes shift are given in the Supporting Information.

(17) Becker, R. S. *Theory and Interpretations of Fluorescence and Phosphorescence*; John Wiley & Sons: New York, 1969.

difference in energy between the Frank–Condon state and the equilibrium state (especially in nonpolar solvents).¹⁷

(18) The Stokes shift of compound **2** was bigger because the longest wavelength vibrational band became smaller than the shorter wavelength one (this depends on the difference of the relative location of the potential energy minima between the excited state and the ground state),¹⁷ and the Stokes shift was calculated between the strongest emission and absorption bands. Thus, it is difficult to compare the Stokes shift in compound **2** with those of compounds **3–5**.

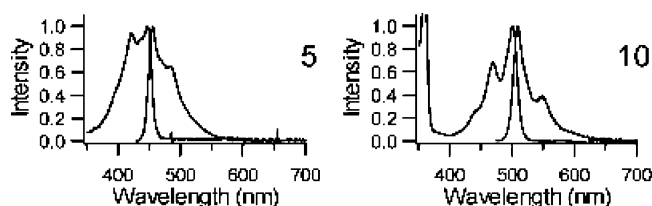


Figure 2. Absorption and fluorescence spectra of compounds 5 and 10.

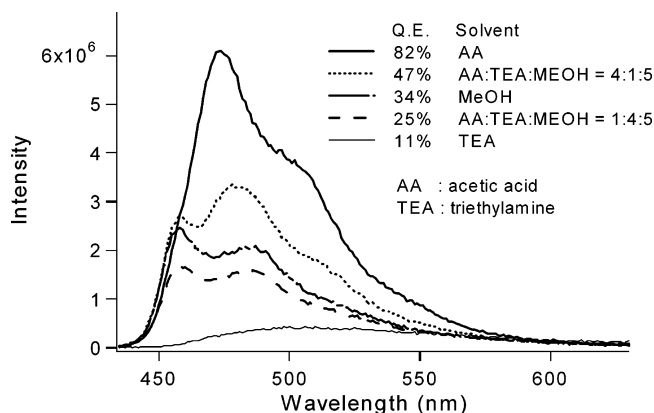


Figure 3. Solvent dependence of fluorescence spectra of compound 11.

The QEs of compounds 2–5 are high in polar solvents, especially in acetic acid.¹⁹ Interestingly, the fluorescence of compounds 2–5, 11, 14, and 15 was enhanced by acid, while that of compounds 6, 7, and 12 was quenched (because the nitrogen of pyridine or quinoline could be protonated), especially compound 11, which behaved as a pK_a sensor (Figure 3). The quantum efficiency changed from 82% (in acetic acid) to 11% (in triethylamine). We will discuss these phenomena later.

Due to their expanded π conjugation, compounds 6 and 7 showed red-shifted spectra (around 20 nm)¹⁶ compared to compound 5. Interestingly the first absorption and fluorescence bands of 6 and 7 are almost identical, which indicates the perturbations to the INI by pyridine and quinoline are essentially identical. Compounds 10, 12, and 13, which have their conjugation extended by ring fusion, showed more red-shifted spectra than 5–7. Among them, 10 shows the most red-shifted spectra. This might be because benzannulated 10 has a more delocalized π -conjugation system than 12 or 13, which have a fused pyridazine.

Crystal Structure. Single crystals of compounds 2, 6, and 7 were grown from CH_2Cl_2 /hexane solution and characterized using X-ray crystallography. To the best of our knowledge, this is the first X-ray crystal structure of the INI ring. Interestingly, and in accord with their aromaticity, all molecules have planar geometries (Figure 4). All bond lengths and angles have the expected values for aromatic compounds (aromatic C^{sp^2} – C^{sp^2} bond length around 1.40 Å), except for, for example, in compound 6, where $\text{C}(5)$ – $\text{C}(6)$ and $\text{C}(11)$ – $\text{C}(12)$ are relatively long (1.452 Å, 1.442 Å, respectively).

The molecules stack along the a axis in compounds 2 and 6 and the b axis in compound 7 to form columnar structures (Figure 5). The crystal has a strong π stacking system, and the distance between planes is only 3.42 Å in 2, 3.44 Å in 6, and

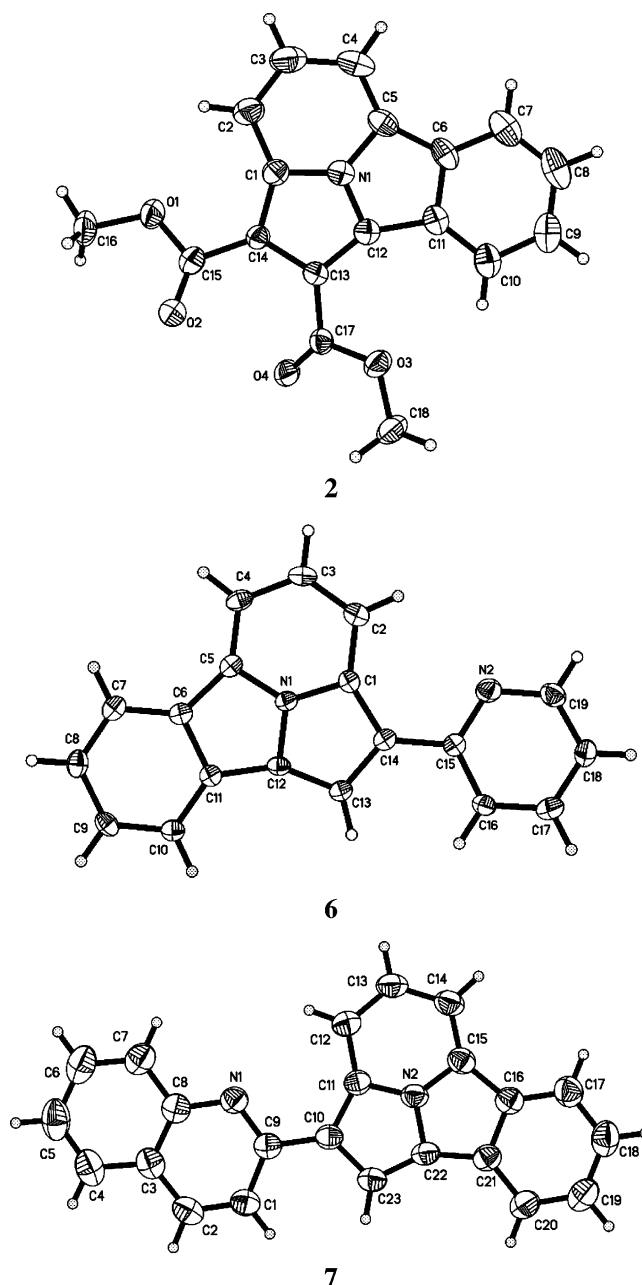
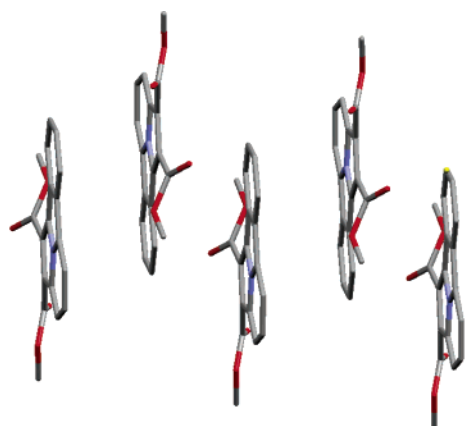


Figure 4. ORTEP diagram of compounds 2, 6, and 7: N(1)–C(12), 1.3677(17); N(1)–C(5), 1.3707(17); N(1)–C(1), 1.3736(17); C(1)–C(2), 1.403(2); C(1)–C(14), 1.429(2); C(2)–C(3), 1.386(2); C(3)–C(4), 1.415(2); C(4)–C(5), 1.376(2); C(5)–C(6), 1.452(2); C(6)–C(7), 1.393(2); C(6)–C(11), 1.4342(19); C(7)–C(8), 1.384(2); C(8)–C(9), 1.404(2); C(9)–C(10), 1.381(2); C(10)–C(11), 1.396(2); C(11)–C(12), 1.4421(19); C(12)–C(13), 1.4006(19); C(13)–C(14), 1.4137(19).

3.46 Å in 7. These values are only slightly larger than that of the interplanar distance in graphite (3.35 Å).²⁰ Remarkably, the distances between columns are also quite small in compounds 6 and 7. The closest intermolecular aromatic ring contacts (C–C, C–N, N–N) between columns are only 3.40 Å along the c axis and 3.67 Å along the b axis in 6 and 3.69 Å along the a axis and 3.72 Å along the c axis in 7. This π -stacking and contact system are strong enough so that the heterocycle is expected to be useful for applications that need high mobility, such as FET devices.²¹

(19) According to ^1H NMR of 5 in acetic acid, a proton bonded to C1 is exchanged with a proton of acetic acid, but 5 remains mostly unprotonated, as evident by the similarity of ^1H NMR before and after addition of acetic acid.

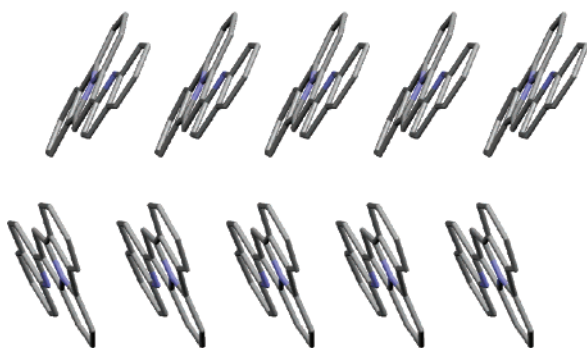
(20) Chung, D. D. L. *J. Mater. Sci.* **2002**, *37*, 1475.



2



6



7

Figure 5. π stacking diagram of compounds 2, 6, and 7.

Electrochemical Studies. Electrochemical data for compounds 2, 3, 5–7, and 9–15 are presented in Table 2. Compounds 2, 12, and 13 showed similar potentials (Figure 6) as the conventional electron transport material²² Alq₃ (oxidation potential, 1.2 to 1.4 V; reduction potential, –1.6 to –1.8 V).

Table 2. Electrochemical Properties of 2–3, 5–7, and 9–15 (in CH₃CN)

compound	E_{ox}^a	E_{red}^b
2	1.24/1.20 ^c	–1.65/–1.77
3	1.11/1.01 ^c	–2.03/–2.25
5	0.81/0.77 ^c	<–2.30 ^e
6	0.80/0.70	–2.11/–2.38
7	0.87/0.73 ^c	–2.18/– ^d
9	0.67/0.61 ^c	<–2.40 ^e
10	0.69/0.50	<–2.40 ^e
11	1.26/– ^d	–1.15/– ^d
12	1.22/1.14	–1.50/–1.62
13	1.34/– ^d	–1.80/–2.01
14	0.81/0.71	<–2.30 ^e
15	0.93/0.78	<–2.40 ^e

^a $E_{ox,pa}/E_{ox,pc}$ (vs/SCE). ^b $E_{red,pa}/E_{red,pc}$ (vs/SCE). ^c Partially reversible. ^d Irreversible. ^e Undetectable.

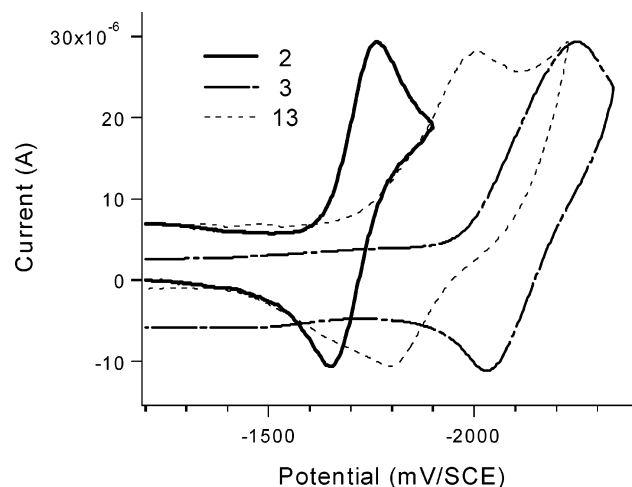


Figure 6. Cyclic voltammetry of compounds 2, 3, and 13.

The reduction potentials of these compounds were also reversible, so we could expect better stability than Alq₃ in reduced states. Alq₃ is known to be unstable in electrochemical studies. As shown in Table 1, compounds 2 and 13 also have a high fluorescence, suggesting that they could be good candidates for alternatives to Alq₃.²³

Oxidation and reduction potentials became smaller as electron-withdrawing ester groups were removed from 2 to 3 and from 3 to 5. The oxidation potential of parent compound 5 is around 0.8 V, which is a desirable energy level for a hole transport material²⁴ in usual organic semiconductor devices, such as OLED. As a result of substitution, when 2 is compared with 3, the reduction potentials change more than oxidation potentials. This indicates the carbonyl at position 1 affects the LUMO level, but the HOMO level is affected to a much lesser extent. Frontier orbital theory²⁵ provides an explanation for such behaviors. The LUMO of the parent INI has a large coefficient at position 1 (11%, Figure 7) so that the substituent effect in this position

(21) (a) Dimitrakopoulos, C. D.; Mascaro, D. J. *IBM J. Res. Dev.* **2001**, *45*, 11. (b) Dimitrakopoulos, C. D.; Malenfant, P. R. L. *Adv. Mater.* **2002**, *14*, 99. (c) Bredas, J. L.; Calbert, J. P.; Filho, D. A. S.; Cornil, J. *Proc. Natl. Acad. Sci. U.S.A.* **2002**, *99*, 5804. (d) Afzali, A.; Dimitrakopoulos, C. D.; Breen, T. L. *J. Am. Chem. Soc.* **2002**, *124*, 8812. (e) Anthony, J. E.; Brooks, J. S.; Eaton, D. L.; Parkin, S. R. *J. Am. Chem. Soc.* **2001**, *123*, 9482. (f) Bredas, J. L.; Beljonne, D.; Cornil, J.; Calbert, J. P.; Shuai, A.; Silbey, R. *Synth. Met.* **2002**, *125*, 107. (g) Anthony, J. E.; Eaton, D. L.; Parkin, S. R. *Org. Lett.* **2002**, *4*, 15. (h) Gruhn, N. E.; Filho, D. A. S.; Bill, T. G.; Malagoli, M.; Coropceanu, V.; Kahn, A.; Brédas, J.-L. *J. Am. Chem. Soc.* **2002**, *124*, 7918.

(22) (a) Posch, P.; Thelakkat, M.; Schmidt, H. W. *Synth. Met.* **1999**, *102*, 1110. (b) Kim, J.; Kim, E.; Choi, J. *J. Appl. Phys.* **2002**, *91*, 1944. (c) Lee, S. T.; Hou, X. Y.; Mason, M. G.; Tang, C. W. *J. Appl. Phys.* **1998**, *72*, 1593. (d) Vestweber, H.; Bassler, H. *J. Appl. Phys.* **2001**, *89*, 3711. (23) Additionally, compounds 2 and 13 also have high luminescence in a solid state, which indicates those have little self-quenching in condensed states. (24) (a) Thelakkat, M.; Shmitz, C.; Hohle, C.; Strohmriegel, P.; Schmidt, H. W.; Hofmann, U.; Schlöter, S.; Haaser, D. *Phys. Chem. Chem. Phys.* **1999**, *1*, 1693. (b) Hu, N.; Xie, S.; Popovic, Z. D.; Ong, B.; Hor, A. M. *Synth. Met.* **2000**, *111*, 421. (25) Fleming, I. *Frontier Orbitals and Organic Chemical Reactions*; John Wiley & Sons: New York, 1976.

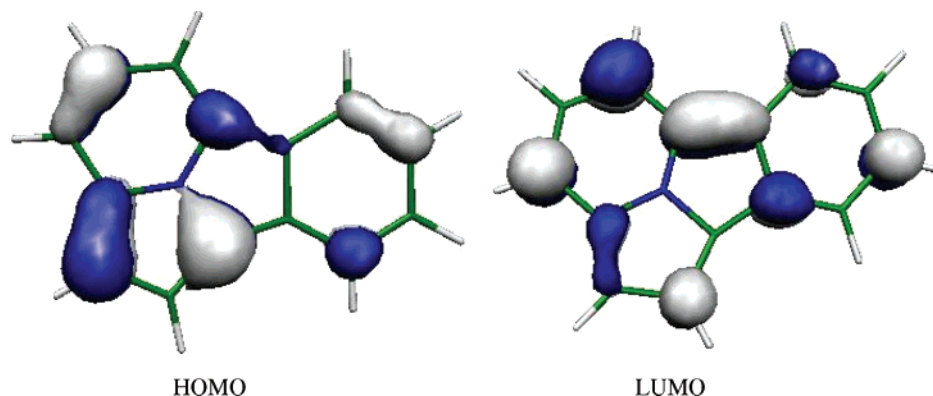


Figure 7. HOMO and LUMO of compound **5** at the MP2/6-31G(d)//B3LYP/6-31G(d) level of theory.

on the reduction potential is large. On the contrary, the HOMO of **INI** has a small coefficient at position 1 (1%) so that the substituent effect on the reduction potential is small.

The oxidation potential did not change from compound **5** to **6** or **7** as a result of a pyridine or a quinoline substitution, but each compound became more reducible due to the enhanced electronegativity of the attached rings. Substituent effects of pyridine and quinoline on redox potentials appear to be similar to the effect on optical spectra (see above).

Because the two **INI** rings in **9** interact through a methylene bridge, the oxidation potential of **9** became smaller (ca. 0.15 eV) compared with **5**, while that of **14** and **15** remained almost the same. A similar effect was observed in optical spectra (red shift about 20 nm) in compound **9**, compared with compounds **5**, **14**, and **15**. The optical spectra of **14** and **15** were almost the same as observed for **5**.

Compounds **10**,^{9f,g} **12**, and **13** have interesting 20π conjugation systems compared with **2** (16π). The oxidation potential of compound **10**^{9f} was lowered by about 0.6 eV due to the fused phenyl ring. On the other hand, the oxidation and reduction potential of compounds **12** and **13** was increased because of a fused electronegative pyridazine ring. From these values, compound **10** is expected to be a good donor or a good hole transport material, and compounds **12** and **13** could be electron transport materials as well as good emitters.

Computational Study of INI. According to the Hückel [$4n + 2$] rule,²⁶ **INI** has 16π electrons and is formally antiaromatic. However, this is a stable planar compound which has NMR signals characteristic for aromatic compounds. To obtain insight into the electronic structure of **INIs**, we have performed density functional calculations at the B3LYP/6-31G(d) level of theory. Compound **5** was shown to be planar by frequency analysis. Examination of calculated geometry helped to solve this dichotomy. In **5**, and in accord with X-ray data, C5a–C5b and C9a–C9b bond lengths are long (1.453 and 1.443 Å, respectively, Figure 8), while all other bonds are normal aromatic bonds. Thus, the π -electrons of **INI** should be considered as two independent aromatic systems, benzene and indolizine, or,

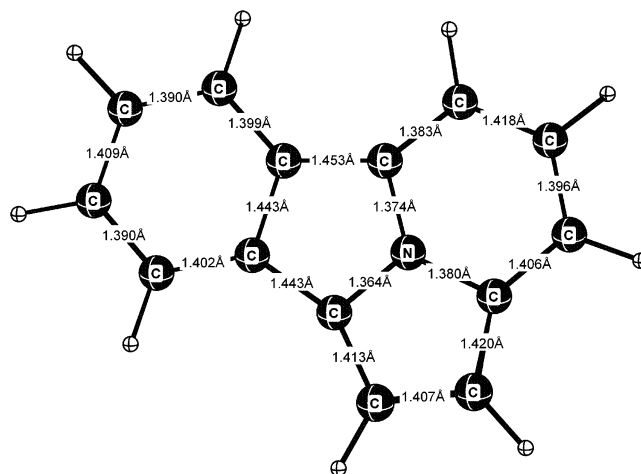
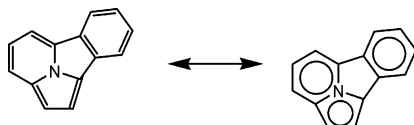


Figure 8. Optimized geometry (B3LYP/6-31G(d)) of **5**.

in other words, **INI** is an aromatic system consisting of $6\pi + 10\pi$ electrons. Similar structural effects are observed in perylene, which is formally a 20π electron system.²⁷

The calculated vertical ionization potential (IP) of **5** is relatively low, 7.0 eV at B3LYP/6-311+G(2df,p)//B3LYP/6-31G(d), only by 0.4 eV higher than the IP of pentacene (6.59 eV) and comparable with that of tetracene (6.97 eV).²⁸ The predicted reorganization energy (calculated as the difference between vertical and adiabatic ionization energies at the B3LYP/6-31G(d)//B3LYP/6-31G(d) level)²⁹ is only 0.092 eV. Both of these values, together with the planar structure of **INI**, make it an attractive candidate for possible applications in field effect transistors.²¹

Protonation Study. As described in the optical properties section, these heterocycles are expected to be basic. Normally protonation of a nitrogen heterocycle occurs at nitrogen, rather than carbon. But heteroaromatic systems in which the nitrogen has three single bonds such as indolizino isindoles are likely to protonate to carbon.³⁰ For example, pyrrole,³¹ indole,³²



(26) Huckel, E. *Z. Phys.* **1932**, 76, 628.

(27) Nather, C.; Bock, H.; Havlas, Z.; Hauck, T. *Organometallics* **1998**, 17, 4707.

(28) Gruhn, N. E.; da Silva Filho, D. A.; Bill, T. G.; Mlagoli, M.; Coropceanu, V.; Kahn, A.; Brédas, J.-L. *J. Am. Chem. Soc.* **2002**, 124, 7918.

(29) The reorganization energy (λ) for self-exchange corresponds to the sum of the geometry relaxation energies upon going from the neutral-state geometry to the charged-state geometry and vice versa. These two portions of λ are typically nearly identical, see: Mlagoli, M.; Brédas, J.-L. *Chem. Phys. Lett.* **2000**, 327, 13.

(30) Fraser, M. *J. Org. Chem.* **1971**, 36, 3087.

(31) Chiang, Y.; Whipple, E. *J. Am. Chem. Soc.* **1963**, 85, 2763.

(32) Hinman, R.; Whipple, E. *J. Am. Chem. Soc.* **1962**, 84, 2534.

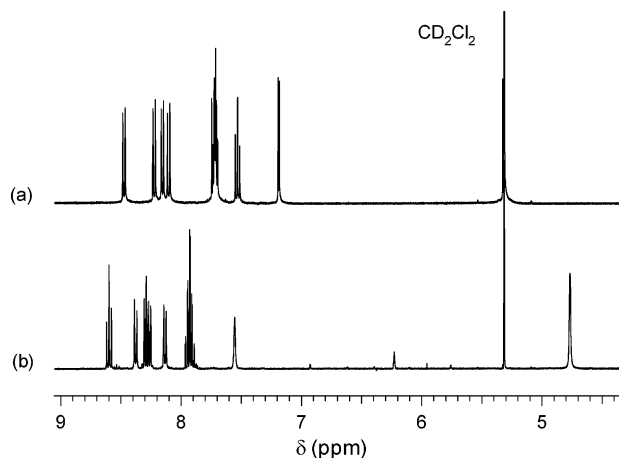


Figure 9. ^1H NMR spectra of (a) compound **5** and (b) protonated compound **5** in CD_2Cl_2 . (a) The sample was measured in CD_2Cl_2 . (b) One drop of the solution (trifluoroacetic acid/trifluoroacetic anhydride = 10/1) was added to sample a. We used anhydride to get rid of water because the protonated **INI(5)** is sensitive to water.

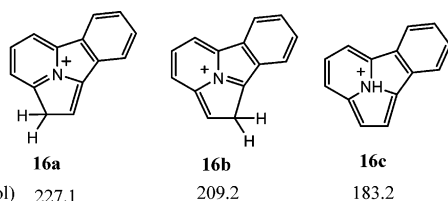


Figure 10. Calculated (at B3LYP/6-311+G(2df,p)//B3LYP/6-31G(d) + ZPVE level of theory) proton affinities of **5**.

isoindole,³³ pyrrole thiazole,³⁴ and indolizine³⁰ were all reported to be protonated at carbon.

Figure 9 shows a ^1H NMR study of the protonation of compound **5** by trifluoroacetic acid. After a trace of acid was added, the NMR spectrum changed from (a) to (b) and a typical singlet peak^{30–34} for protonation was found at 4.77 ppm for two protons.¹⁹ From these NMR spectra³⁵ the protonation site can be deduced as the position 1 or 2. Gas-phase protonation of **5** was studied computationally in order to determine the protonation site.

In agreement with experimental results, **5** is predicted to protonate easily, the calculated proton affinity is 227.1 kcal/mol (in gas phase, at B3LYP/6-311+G(2df,p)//B3LYP/6-31G(d) + ZPVE). For comparison, gas-phase proton affinity of tetracene is 216.4 kcal/mol,³⁶ of pentacene it is 225.7 kcal/mol,³⁷ and that of pyrrole is 222 kcal/mol.³⁶ Calculations also reveal the most preferred protonation place (Figure 10). In agreement with the aromatic character of **INI**, protonation of **5** on nitrogen is unfavorable (**16c**, 183.2 kcal/mol). Additionally, the HOMO of **5** is delocalized over the aromatic system and the coefficient on nitrogen is only 2% (Figure 7). Expectedly, position 2 has

Table 3. Electroluminescence Data for the Compounds **3**, **6**, **7**, and **13**

	compound 3	compound 6	compound 7	compound 13
V_{th} (V) ^a	6.0	7.0	7.0	6.2
max luminance (cd/m^2)	5674	7009	11390	8328
power efficiency, ^b 100 (lm/W)	0.94	1.08	1.24	1.57
voltage ^b 100 (V)	9.0	9.8	9.8	9.2
L/J ^c (cd/A)	2.70	3.37	3.90	4.59
peak (FWHM ^d) (nm)	450(59)	486(51)	486(53)	488(40)
CIE _x	0.165	0.169	0.177	0.175
CIE _y	0.188	0.463	0.449	0.439

^a Turn on voltage. ^b Taken at 100 cd/m^2 . ^c Current efficiency at 100 cd/m^2 . ^d Full width half-maximum.

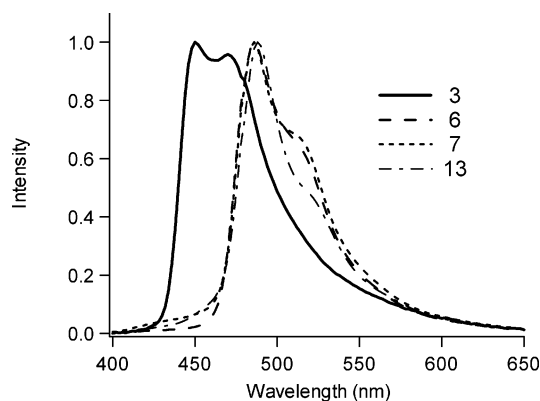
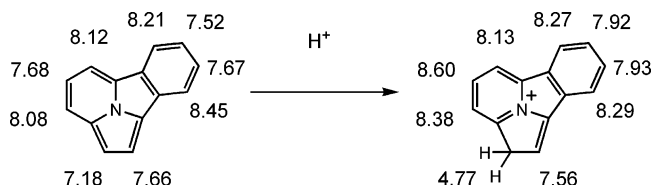


Figure 11. Comparison of the EL spectra of compounds **3**, **6**, **7**, and **13**.

a high HOMO coefficient of 17% and has the highest proton affinity, leading to an aromatic pyridinium cation.

From these results we can assign the structure of the protonated compound and chemical shifts δ (ppm) of ^1H NMR as shown in the following diagram.³⁸



Characteristics of Light-Emitting Devices. Using the phosphors discussed above, we prepared efficient OLEDs (from heterocycles **3**, **6**, **7**, and **13**), which emit from blue to green. The organic EL devices were fabricated according to the procedure previously reported.³⁹ The OLEDs comprised four organic layers between ITO and cathode: ITO/CuPc (copper phthalocyanine, 10 nm)/CPB (4,4'-bis(carbazol-9-yl)biphenyl, 60 nm)/**INI**s (30 nm)/Salq (bis(2-methyl-8-quinolinolato-N1,-O8)(triphenylsilanolato)aluminum, 10 nm)/Alq₃ (35 nm)/MgF₂.

The most important parameters are compiled in Table 3 and the voltage, current density, luminance characteristics and EL spectra are displayed in Figures 11–13. The observed EL spectra were almost identical with PL spectra, which means the luminescences originated from the heterocycles and holes were efficiently blocked by Salq to prevent Alq₃ from emitting by itself.

(33) Bender, C. O.; Bonnett, R. *Chem. Commun.* **1966**, 7, 198.

(34) Malloy, B.; Reid, D. J. *Chem. Soc.* **1965**, 4369.

(35) NMR of protonated compound **5**. ^1H NMR (500 MHz, CD_2Cl_2): δ 8.60 (dd, J = 8.0, 7.8 Hz, 1H), 8.38 (d, J = 8.0 Hz, 1H), 8.29 (ddd, J = 7.6, 1.6, 0.9 Hz, 1H), 8.27 (ddd, J = 7.6, 1.6, 0.9 Hz, 1H), 8.13 (d, J = 7.8 Hz, 1H), 7.93 (td, J = 7.6, 1.6 Hz, 1H), 7.91 (td, J = 7.6, 1.6 Hz, 1H), 7.56 (s, 1H), 4.77 (s, 2H). ^{13}C NMR (125 MHz, CD_2Cl_2): δ 143.2, 133.3, 132.1, 124.7, 124.4, 124.3, 120.4, 118.2, 44.8.

(36) Lias, S. G.; Bartmess, J. E.; Liebman, J. F.; Holmes, J. L.; Levin, R. D.; Mallard, W. G. In *Ion Energetics Data*; Mallard, W. G., Linstrom, P. J., Eds.; NIST Chemistry WebBook, NIST Standard Reference Database No. 69, July 2001; National Institute of Standards and Technology: Gaithersburg, MD, 2001 (<http://webbook.nist.gov>).

(37) Notario, R.; Abboud, J.-L. M. *J. Phys. Chem. A* **1998**, 102, 5290.

(38) The pairs of (1,3-H), (6, 9-H), and (7,8-H) in protonated compound **5** are changeable.

(39) Sato, Y.; Ogata, T.; Ichinosawa, S.; Murata, Y. *Synth. Met.* **1997**, 91, 103.

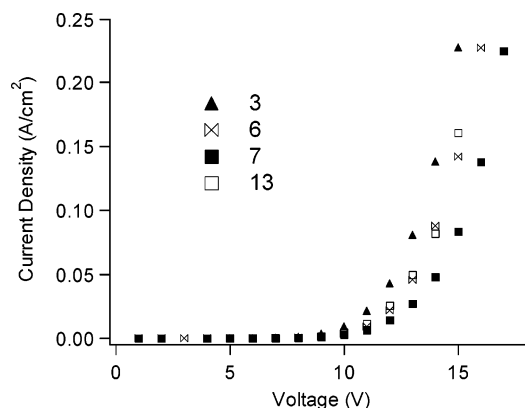


Figure 12. Applied field vs current density characteristics of compounds **3**, **6**, **7**, and **13**.

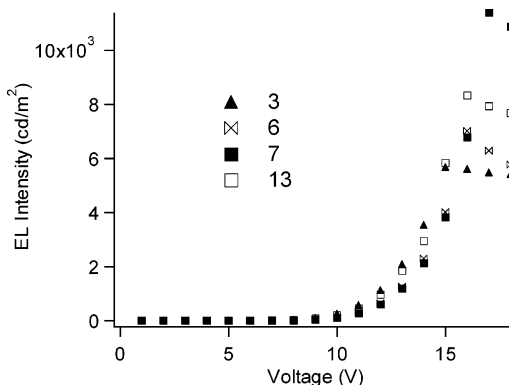


Figure 13. Applied field vs EL intensity characteristics of compounds **3**, **6**, **7**, and **13**.

It is interesting to note that the device based on **3** emits beautiful blue light, based on its CIE (Commission Internationale d'Eclairage) chromaticity coordinates (x , y : 0.165, 0.188) and the spectra for all devices are relatively sharp, which suggests the emitting colors are pure. The brightness of the device reached as high as 10^4 cd/m². The stability (color and brightness) under the highest voltage was similar to that of Coumarin 30. The performance (especially in efficiency) for all compounds appears to be promising when compared to the blue-emitting devices reported recently.⁴⁰

Conclusion

On the basis of the indolizino–isoindole unit, 14 heterocycles have been prepared, and their optical, electronic properties and crystal structures have been studied. The heterocycles have blue or green emission, and their quantum efficiency was found to be as high as 90%. The brightness of the light-emitting device reached as high as 10^4 cd/m², and **3** emits “perfect” blue light. We also found some heterocycles could become alternatives to Alq₃ because they have almost the same energy potential levels and have high luminescence, not only in solution but also in

the solid states. As for electronic properties, we could interpret the interesting $16\pi = 10\pi + 6\pi$ conjugation system from X-ray structure and DFT calculations. An NMR-based protonation study revealed the indolizino–isoindole was protonated at the 2-carbon.

Further research, including incorporation as transition metal chelates, is in progress in our laboratory.

Experimental Section

Synthesis of Pyrido[2,1-*a*]isoindole (1). This compound was prepared according to a modified literature procedure.^{10,11} First 2-bromopyridine was allowed to react with benzyl bromide to afford 1-benzyl-2-bromopyridinium bromide.¹⁰ Then this salt (in 2% of hydrobromic acid) was irradiated with a halogen lamp to afford 6*H*-pyrido[2,1-*a*]isoindolylum bromide. The resulting bromide was aromatized by aqueous Na₂CO₃ to afford pyrido[2,1-*a*]isoindole (**1**)¹¹ quantitatively, which was used freshly for the next steps.

Indolizino[3,4,5-*ab*]isoindole-1,2-dicarboxylic Acid Dimethyl Ester (2). This compound was prepared according to the literature method.^{9a} Recrystallization from CH₂Cl₂/hexane afforded a fine yellow solid in 65% yield. mp 182.0–183.0 °C (lit. 184–185 °C.^{9a} lit. 175 °C.^{9c} lit. 190 °C.^{9b}). ¹H NMR (CDCl₃): δ 8.46 (d, J = 8.6 Hz, 1H), 8.43 (d, J = 9.0 Hz, 1H), 8.35 (d, J = 8.0 Hz, 1H), 8.07 (d, J = 8.0 Hz, 1H), 8.21 (dd, J = 9.0, 8.6 Hz, 1H), 7.74 (t, J = 8.0 Hz, 1H), 7.62 (t, J = 8.0 Hz, 1H), 4.17 (s, 3H), 4.04 (s, 3H). ¹³C NMR (CDCl₃): δ 165.0, 164.4, 130.7, 130.1, 129.8, 129.6, 129.3, 125.6, 125.0, 124.7, 122.4, 122.1, 118.5, 118.3, 110.0, 109.0, 52.4, 51.6. MS (EI⁺): m/z 307.1 (M⁺). Anal. Calcd. for C₁₈H₁₃NO₄: C, 70.35; H, 4.26; N, 4.56. Found: C, 70.50; H, 4.30; N, 4.60. IR (DRIFT): ν (C=O) 1731, 1701 cm^{−1}.

Indolizino[3,4,5-*ab*]isoindole-2-carboxylic Acid Methyl Ester (3). This adduct was prepared according to a procedure similar to that for compound **2**, using methyl acrylate instead of methyl maleate. In 50% yield. mp 118.0–119.0 °C (lit. 119–120 °C.^{9b}). ¹H NMR (CDCl₃): δ 8.48 (d, J = 8.4 Hz, 1H), 8.38 (d, J = 8.0 Hz, 1H), 8.19 (d, J = 8.0 Hz, 1H), 8.11 (s, 1H), 8.09 (d, J = 7.4 Hz, 1H), 7.88 (dd, J = 8.4, 7.4 Hz, 1H), 7.82 (t, J = 8.0 Hz, 1H), 7.71 (t, J = 8.0 Hz, 1H), 4.03 (s, 3H). ¹³C NMR (CDCl₃): δ 165.8, 130.3, 130.2, 129.7, 129.5, 128.9, 124.3, 123.9, 122.7, 122.5, 120.2, 116.8, 114.4, 110.5, 108.9, 51.3. MS (EI⁺): m/z 249.1 (M⁺). Anal. Calcd for C₁₆H₁₁NO₂: C, 77.10; H, 4.45; N, 5.62. Found: C, 77.37; H, 4.43; N, 5.38. IR (DRIFT): ν (C=O) 1693 cm^{−1}.

Indolizino[3,4,5-*ab*]isoindole-1,2-dicarboxylic Acid (4). This compound was prepared on the basis of a literature method.^{9c} Indolizino[3,4,5-*ab*]isoindole-1,2-dicarboxylic acid dimethyl ester (2; 0.25 g, 0.82 mmol) was dissolved in THF (5 mL) and aqueous NaOH (10%; 10 mL) was added. The mixture was refluxed for 5 h. After the mixture was cooled to room temperature, aqueous HCl (20%) was added until pH < 3. A yellow precipitate was collected and washed with water (2 × 5 mL) and dried in vacuo to obtain a yellow solid (0.19 g, 0.68 mmol) in 84% yield. mp 293 °C (decomp). ¹H NMR (CDCl₃): δ 8.75 (d, J = 8.1 Hz, 1H), 8.58 (d, J = 8.1 Hz, 1H), 8.49 (d, J = 8.5 Hz, 1H), 8.48 (d, J = 7.4 Hz, 1H), 8.08 (dd, J = 8.5, 7.4 Hz, 1H), 7.82 (t, J = 8.1 Hz, 1H), 7.71 (t, J = 8.1 Hz, 1H). ¹³C NMR (CDCl₃): δ 169.8, 165.7, 131.6, 130.6, 130.4, 130.3, 129.6, 127.9, 127.2, 123.9, 123.8, 119.6, 112.5, 107.3. MS (EI⁺): m/z 279.1 (M⁺). Anal. Calcd for C₁₆H₉NO₄: C, 68.82; H, 3.25; N, 5.02. Found: C, 68.40; H, 3.29; N, 5.20. IR (DRIFT): ν (C=O) 1695 cm^{−1}, ν (OH) 2300–3600 cm^{−1}.

Indolizino[3,4,5-*ab*]isoindole (5). This compound was prepared on the basis of a literature method.^{9c} Quinoline (30 mL), indolizino[3,4,5-*ab*]isoindole-1,2-dicarboxylic acid (**4**; 0.30 g, 1.25 mmol), and copper chromite (0.67 g, 3.75 mmol) were charged in a round-bottom flask, and the mixture was stirred for 4 h at 210 °C under N₂. After the mixture was cooled to room temperature, CH₂Cl₂ (50 mL) was added and a black inorganic solid was removed by filtration. The solvents were

(40) (a) Hosokawa, C.; Higashi, H.; Nakamura, H.; Kusumoto, T. *Appl. Phys. Lett.* **1995**, *67*, 3853. (b) Gao, Z.; Lee, C. S.; Bello, I.; Lee, S. T.; Chen, R. M.; Luh, T. Y.; Shi, J.; Wang, C. W. *Appl. Phys. Lett.* **1999**, *74*, 865. (c) Balasubramaniam, E.; Tao, Y. T.; Danel, A.; Tomasik, P. *Chem. Mater.* **2000**, *12*, 2788. (d) Leusng, L.; Lo, W. Y.; So, S. K.; Lee, K. M.; Choi, W. K. *J. Am. Chem. Soc.* **2000**, *122*, 5640. (e) Tao, Y. T.; Balasubramaniam, E.; Danel, A.; Jarosz, B.; Tomasik, P. *Chem. Mater.* **2001**, *13*, 1207. (f) Ko, C. W.; Tao, Y. T.; Danel, A.; Kreminska, L.; Tomasik, P. *Chem. Mater.* **2001**, *13*, 2441. (g) Thomas, K. R.; Lin, J. T.; Tao, Y. T.; Ko, C. W. *Chem. Mater.* **2002**, *14*, 1354.

removed under vacuum, and the residue was chromatographed on silica gel with $\text{CH}_2\text{Cl}_2/\text{hexane} = 1/1$. Recrystallization from $\text{CH}_2\text{Cl}_2/\text{hexane}$ afforded a fine yellow solid (0.13 g, 0.68 mmol) in 54% yield. mp 85.0–86.0 °C (lit. 75 °C^{9c}). ^1H NMR (CDCl_3): δ 8.45 (dt, $J = 8.0$, 1.0 Hz, 1H), 8.21 (dt, $J = 8.1$, 1.0 Hz, 1H), 8.12 (d, $J = 7.4$ Hz, 1H), 8.08 (d, $J = 8.1$ Hz, 1H), 7.68 (dd, $J = 8.1$, 7.4 Hz, 1H), 7.67 (td, $J = 8.0$, 1.0 Hz, 1H), 7.66 (d, $J = 4.1$ Hz, 1H), 7.52 (td, $J = 8.0$, 1.0 Hz, 1H), 7.18 (d, $J = 4.1$ Hz, 1H). ^{13}C NMR (CDCl_3): δ 129.6, 128.8, 128.3, 127.9, 127.8, 122.4, 122.3, 121.9, 119.2, 119.1, 115.3, 112.6, 107.9, 105.5 MS (EI⁺): m/z 191.1 (M^+). Anal. Calcd for $\text{C}_{14}\text{H}_9\text{N}$: C, 87.93; H, 4.74; N, 7.32. Found: C, 87.82; H, 4.57; N, 7.22.

2-Pyridin-2-yl-2a,3-dihydroindolizino[3,4,5-*ab*]isoindole (6a). Pyridol[2,1-*a*]isoindole (**1**) (0.80 g, 4.8 mmol) was dissolved in degassed $\text{ClCH}_2\text{CH}_2\text{Cl}$ (50 mL). To this solution, 2-ethynylpyridine (0.59 g, 5.7 mmol) in $\text{ClCH}_2\text{CH}_2\text{Cl}$ (10 mL) was added dropwise and the mixture was refluxed for 6 h. The mixture was diluted with CH_2Cl_2 (20 mL), washed with H_2O (50 mL), and dried over Na_2SO_4 . The solvent was evaporated and the residue was chromatographed on silica gel with hexane/ $\text{CH}_2\text{Cl}_2 = 4/1$. Recrystallization from $\text{CH}_2\text{Cl}_2/\text{hexane}$ afforded green crystals (0.70 g, 2.6 mmol) in 54% yield. mp 146.0–147.5 °C. ^1H NMR (CDCl_3): δ 8.52 (dd, $J = 6.5$, 1.1 Hz, 1H), 7.63 (td, $J = 7.5$, 1.9 Hz, 1H), 7.56 (dd, $J = 7.5$, 1.0 Hz, 1H), 7.51 (dd, $J = 7.5$, 1.1 Hz, 1H), 7.43 (dd, $J = 7.5$, 0.9 Hz, 1H), 7.37 (td, $J = 7.5$, 0.9 Hz, 1H), 7.31 (dd, $J = 9.0$, 3.0 Hz, 1H), 7.21 (td, $J = 7.5$, 1.1 Hz, 1H), 7.01 (ddd, $J = 7.5$, 6.5, 1.0 Hz, 1H), 6.71 (s, 1H), 5.89 (ddd, $J = 9.0$, 6.4, 2.5 Hz, 1H), 4.89 (dd, $J = 15.7$, 6.4 Hz, 1H), 2.86 (dt, $J = 16.4$, 6.4 Hz, 1H), 2.38 (dddd, $J = 15.7$, 16.4, 3.0, 2.5 Hz, 1H). ^{13}C NMR (CDCl_3): δ 155.7, 149.3, 145.3, 136.1, 134.8, 134.7, 128.3, 125.2, 124.3, 124.1, 123.1, 122.2, 120.6, 119.8, 119.5, 119.4, 98.8, 52.9, 27.3. MS (EI⁺): m/z 270.1 (M^+). Anal. Calcd for $\text{C}_{19}\text{H}_{14}\text{N}_2$: C, 84.42; H, 5.22; N, 10.36. Found: C, 84.56; H, 5.03; N, 10.58.

2-Pyridin-2-ylindolizino[3,4,5-*ab*]isoindole (6). Chlorobenzene (30 mL), 2-pyridin-2-yl-2a,3-dihydroindolizino[3,4,5-*ab*]isoindole (**6a**) (0.30 g, 1.1 mmol) and sulfur (0.50 g, 16 mmol) were charged in a round-bottom flask, and the mixture was refluxed for 10 h. The solvent was evaporated, and the residue was chromatographed on silica gel with hexane/ethyl acetate = 5/1. Recrystallization from $\text{CH}_2\text{Cl}_2/\text{hexane}$ afforded a fine yellow solid (0.17 g, 0.66 mmol) in 59% yield. mp 111.5–112.5 °C. ^1H NMR (CD_2Cl_2): δ 8.84 (d, $J = 8.3$ Hz, 1H), 8.68 (d, $J = 4.1$ Hz, 1H), 8.44 (d, $J = 8.0$ Hz, 1H), 8.24 (d, $J = 8.0$ Hz, 1H), 8.14 (d, $J = 8.0$ Hz, 1H), 8.14 (s, 1H), 7.89 (d, $J = 8.0$ Hz, 1H), 7.84 (dd, $J = 8.0$, 8.3 Hz, 1H), 7.75 (dd, $J = 8.0$, 7.2 Hz, 1H), 7.73 (dd, $J = 8.0$, 7.3 Hz, 1H), 7.55 (dd, $J = 8.0$, 7.2 Hz, 1H), 7.11 (dd, $J = 7.2$, 4.1 Hz, 1H). ^{13}C NMR (CDCl_3): δ 156.2, 149.9, 136.8, 130.2, 129.8, 129.2, 128.6, 127.7, 123.8, 123.7, 122.9, 122.0, 121.2, 120.2, 120.0, 119.9, 118.5, 110.5, 109.3. MS (EI⁺): m/z 268.1 (M^+). Anal. Calcd for $\text{C}_{19}\text{H}_{12}\text{N}_2$: C, 85.05; H, 4.51; N, 10.44. Found: C, 85.00; H, 4.25; N, 10.43.

2-Quinolin-2-yl-2a,3-dihydroindolizino[3,4,5-*ab*]isoindole (7a). This compound was prepared in a procedure similar to that of compound **6a**, using 2-ethynylquinoline instead of 2-ethynylpyridine (prepared according to the literature method⁴¹). In 57% yield. mp 148.0–150.0 °C. ^1H NMR (CDCl_3): δ 8.20 (d, $J = 8.2$ Hz, 1H), 7.99 (dd, $J = 8.0$, 1.0 Hz, 1H), 7.76 (dd, $J = 8.0$, 1.0 Hz, 1H), 7.75 (d, $J = 8.4$ Hz, 1H), 7.71 (d, $J = 8.2$ Hz, 1H), 7.66 (dd, $J = 8.4$, 7.6 Hz, 1H), 7.60 (d, $J = 7.6$ Hz, 1H), 7.56 (dd, $J = 8.9$, 3.0 Hz, 1H), 7.45 (td, $J = 8.0$, 1.0 Hz, 2H), 7.39 (td, 7.6, 1.3 Hz, 1H), 6.87 (s, 1H), 5.98 (ddd, $J = 8.9$, 6.5, 2.4 Hz, 1H), 4.95 (dd, $J = 15.8$, 6.5 Hz, 1H), 2.90 (dt, $J = 16.3$, 6.5 Hz, 1H), 2.43 (dddd, $J = 16.3$, 15.8, 3.1, 2.4 Hz, 1H). MS (EI⁺): m/z 320.1 (M^+). Anal. Calcd for $\text{C}_{23}\text{H}_{16}\text{N}_2$: C, 86.22; H, 5.03; N, 8.74. Found: C, 86.04; H, 4.84; N, 8.40.

2-Quinolin-2-ylindolizino[3,4,5-*ab*]isoindole (7). This compound was prepared in a procedure similar to that of compound **6**, using **7a**

instead of **6a**. In 42% yield. mp 192.0–193.0 °C. ^1H NMR (CD_2Cl_2): δ 9.17 (d, $J = 8.3$ Hz, 1H), 8.47 (dd, $J = 8.0$, 0.9 Hz, 1H), 8.27 (d, $J = 8.9$ Hz, 1H), 8.26 (s, 1H), 8.21 (d, $J = 8.7$ Hz, 1H), 8.20 (d, $J = 7.3$ Hz, 1H), 8.16 (d, $J = 8.4$ Hz, 1H), 8.08 (d, $J = 8.7$ Hz, 1H), 7.93 (dd, $J = 8.4$, 7.3 Hz, 1H), 7.82 (dd, $J = 8.0$, 1.2 Hz, 1H), 7.76 (ddd, $J = 8.0$, 7.1, 1.0 Hz, 1H), 7.72 (ddd, $J = 8.3$, 6.9, 1.2 Hz, 1H), 7.57 (ddd, $J = 8.9$, 7.1, 0.9 Hz, 1H), 7.47 (ddd, $J = 8.0$, 6.9, 1.2 Hz, 1H). ^{13}C NMR (CD_2Cl_2): δ 155.4, 148.4, 135.7, 129.5, 129.2, 129.1, 128.7, 128.5, 128.0, 127.2, 126.1, 124.7, 123.1, 122.3, 122.2, 121.9, 120.7, 120.7, 119.4, 118.6, 118.5, 110.5, 108.9. MS (EI⁺): m/z 318.1 (M^+). Anal. Calcd for $\text{C}_{23}\text{H}_{14}\text{N}_2$: C, 86.77; H, 4.43; N, 8.80. Found: C, 85.84; H, 4.13; N, 8.79.

2-Bromoindolizino[3,4,5-*ab*]isoindole (8). Indolizino[3,4,5-*ab*]isoindole (**5**) (0.25 g, 1.3 mmol) was dissolved in distilled CH_2Cl_2 (10 mL). To this solution Br_2 (0.21 g, 1.3 mmol) in CH_2Cl_2 (5 mL) was added dropwise at -10 °C, and the mixture was stirred for 1 h at 0 °C. The solution was diluted with CH_2Cl_2 (50 mL), and aqueous NaHCO_3 (50 mL) were added. The organic layer was extracted, washed with H_2O (2×50 mL), and dried over Na_2SO_4 . The solvents were evaporated, and the residue was chromatographed on silica gel with hexane. Recrystallization from $\text{CH}_2\text{Cl}_2/\text{hexane}$ afforded a yellow solid (0.20 g, 0.96 mmol) in 74% yield. mp 88.0–89.5 °C. ^1H NMR (CD_2Cl_2): δ 8.45 (dd, $J = 8.1$, 1.0 Hz, 1H), 8.18 (dd, $J = 8.1$, 1.0 Hz, 1H), 8.14 (d, $J = 7.3$ Hz, 1H), 8.03 (d, $J = 8.4$ Hz, 1H), 7.77 (dd, $J = 8.4$, 7.3 Hz, 1H), 7.73 (td, $J = 8.1$, 1.0 Hz, 1H), 7.69 (s, 1H), 7.54 (td, $J = 8.1$, 1.0 Hz, 1H). ^{13}C NMR (CD_2Cl_2): δ 129.3, 128.4, 128.3, 126.5, 123.2, 122.6, 121.2, 128.7, 120.2, 119.4, 114.1, 113.8, 108.8, 91.0. MS (EI⁺): m/z 269.0 (M^+). Anal. Calcd for $\text{C}_{14}\text{H}_8\text{BrN}$: C, 62.25; H, 2.99; N, 5.19, Br, 29.58. Found: C, 62.01; H, 3.15; N, 4.81, Br, 4.81.

Methylene Bis(indolizino[3,4,5-*ab*]isoindol-2-yl)Benzene (9). Dry THF (5 mL), indolizino[3,4,5-*ab*]isoindole (**5**) (0.17 g, 1.0 mmol), benzaldehyde (75 mg, 0.75 mmol), and *p*-toluenesulfonic acid (5 mg) was charged in a round-bottom flask, and the solution was stirred at 50 °C for 3 h. The mixture was diluted with Et_2O (30 mL), and aqueous NaHCO_3 (30 mL) was added. The organic layer was extracted, washed with H_2O (2×50 mL), and dried over Na_2SO_4 . The solvents were evaporated, and the residue was chromatographed on alumina with hexane. Recrystallization from $\text{CH}_2\text{Cl}_2/\text{hexane}$ afforded a yellow solid 0.20 g (0.96 mmol) in 22% yield. mp 158 °C (decomp). ^1H NMR (CD_2Cl_2): δ 8.45 (d, $J = 8.0$ Hz, 2H), 8.12 (d, $J = 8.0$ Hz, 2H), 8.11 (d, $J = 7.5$ Hz, 2H), 7.67 (t, $J = 8.0$ Hz, 2H), 7.66 (d, $J = 8.2$ Hz, 2H), 7.59 (d, $J = 7.3$ Hz, 2H), 7.56 (s, 1H), 7.51 (dd, $J = 8.2$, 7.3 Hz, 2H), 7.50 (dd, $J = 7.5$, 7.3 Hz, 2H), 7.36 (t, $J = 8.0$ Hz, 2H), 7.30 (t, $J = 7.3$ Hz, 2H), 6.79 (s, 1H). MS (EI⁺): m/z 470.2 (M^+). Anal. Calcd for $\text{C}_{35}\text{H}_{22}\text{N}_2$: C, 89.33; H, 4.71; N, 5.95. Found: C, 89.30; H, 4.32; N, 5.20.

Benzo[1',2'-1,2]indolizino[3,4,5-*ab*]isoindole (10). 2,2,6,6-Tetramethylpiperidine (1.41 g, 10 mmol) was dissolved in dry THF (10 mL), and 2.5 *M* *n*-butyllithium solution in hexane (4 mL, 20 mmol) was added dropwise at 0 °C. The solution turned yellow. The mixture was stirred for 30 min at 0 °C (solution A). Dry THF (60 mL), pyridol[2,1-*a*]isoindole (**1**) (1.25 g, 7.5 mmol), and bromobenzene (0.63 g, 4.0 mmol) were charged in another round-bottom flask, and solution A was added dropwise at -78 °C under N_2 to give a black solution. After stirring 1 h at -78 °C, the solution was diluted with Et_2O (20 mL), washed with aqueous NH_4Cl (20 mL), washed with H_2O (20 mL), and dried over Na_2SO_4 . The solvent was evaporated, and the black residue was chromatographed on silica gel with hexane/ $\text{CH}_2\text{Cl}_2 = 4/1$. Recrystallization from $\text{CH}_2\text{Cl}_2/\text{hexane}$ afforded an orange solid (60 mg, 0.25 mmol) in 6.6% yield. mp 169.0–171.0 °C (lit. 175–176 °C⁹ⁱ). ^1H NMR (CD_2Cl_2): δ 8.57 (dt, 8.2, 1 Hz, 2H), 8.56 (d, 7.8 Hz, 2H), 8.42 (dt, 8.2, 1.0 Hz, 2H), 7.90 (t, 7.8 Hz, 1H), 7.76 (ddd, 8.1, 7.0, 1.0 Hz, 2H), 7.50 (ddd, 8.1, 7.0, 1.0 Hz, 2H). MS (EI⁺): m/z 241.1 (M^+). Anal. Calcd for $\text{C}_{18}\text{H}_{11}\text{N}$: C, 89.60; H, 4.60; N, 5.81. Found: C, 89.83; H, 4.87; N, 5.85.

(41) Sakamoto, T.; Shirakawa, M.; Kondo, Y.; Yamanaka, H. *Synthesis* **1983**, 4, 313.

2,3-Hydropyridazino[4',5':1,2]indolizino[3,4,5-*ab*]isoindole-1,4-dione (11). Ethanol (20 mL), chlorobenzene (20 mL), indolizino[3,4,5-*ab*]isoindole-1,2-dicarboxylic acid dimethyl ester (**2**; 0.31 g, 1.0 mmol), and hydrazine (1 mL) were charged in a round-bottom flask, and the mixture was refluxed for 5 days. The yellow precipitate was collected and washed with CH₂Cl₂ (10 mL), followed by ethanol (10 mL), and dried in vacuo to obtain a yellow solid (0.24 g, 0.87 mmol) in 87% yield. mp 346 °C (decomp). ¹H NMR (DMSO-*d*₆): δ 8.80 (d, *J* = 7.4 Hz, 1H), 8.75 (dd, *J* = 8.0, 0.9 Hz, 1H), 8.66 (d, *J* = 8.2 Hz, 1H), 8.54 (dd, *J* = 8.0, 0.9 Hz, 1H), 8.18 (td, *J* = 8.0, 0.9 Hz, 1H), 7.89 (td, *J* = 8.0, 0.9 Hz, 1H), 7.71 (td, *J* = 8.0, 0.9 Hz, 1H) 6.5–5.5 (br, 2H). ¹³C NMR (DMSO-*d*₆): δ 147.8, 129.7, 129.4, 129.1, 125.1, 124.3, 123.9, 121.5, 117.6, 113.8. HRMS. Calcd for C₁₆H₉N₃O₂: 275.0695. Found: 275.0690. IR: ν (NH) 2300–3500 cm⁻¹, ν (C=O) 1651, 1660 cm⁻¹.

1,4-Dichloropyridazino[4',5':1,2]indolizino[3,4,5-*ab*]isoindoles (12). Phosphorus oxychloride (3 mL), 2,3-hydropyridazino[4',5':1,2]indolizino[3,4,5-*ab*]isoindole-1,4-dione (**11**) (0.20 g, 0.73 mmol), PCl₅ (0.30 g, 1.45 mmol), and a drop of dimethylformamide (DMF) were charged in a round-bottom flask. The solution was stirred at 130 °C for 4 h, whereupon an orange solid precipitated. The mixture was cooled to room temperature, and POCl₃ was evaporated in vacuo. The residue was washed with CH₂Cl₂ (20 mL), followed by EtOH (20 mL), and dried in vacuo to obtain a brown solid (0.20 g, 0.63 mmol) in 86% yield. mp 153 °C (decomp). ¹H NMR (DMSO-*d*₆): δ 9.09 (d, *J* = 7.7 Hz, 1H), 9.01 (d, *J* = 8.3 Hz, 1H), 8.79 (d, *J* = 8.0 Hz, 1H), 8.71 (d, *J* = 8.0 Hz, 1H), 8.41 (t, *J* = 8.0 Hz, 1H), 7.90 (dd, *J* = 8.3, 7.7 Hz, 1H), 7.75 (t, *J* = 8.0 Hz, 1H). HRMS. Calcd for C₁₆H₇Cl₂N₃: 311.0017. Found: 311.0012.

1,4-Diphenoxypyridazino[4',5':1,2]indolizino[3,4,5-*ab*]isoindoles (13). Phenol (113 mg, 1.2 mmol), 1,4-dichloropyridazino[4',5':1,2]indolizino[3,4,5-*ab*]isoindoles (**12**) (94 mg, 0.30 mmol), K₂CO₃ (300 mg), and DMF (5 mL) were charged in a round-bottom flask, and the mixture was refluxed for 3 days. The mixture was diluted with Et₂O (200 mL), washed with H₂O (40 mL), and dried over Na₂SO₄. The solvent was evaporated, and the residue was chromatographed on alumina with CH₂Cl₂. Recrystallization from CH₂Cl₂/hexane afforded an orange solid (70 mg, 0.16 mmol) in 55% yield. mp 224.0–224.5 °C. ¹H NMR (CDCl₃): δ 8.78 (d, *J* = 8.1 Hz, 1H), 8.64 (d, *J* = 7.5 Hz, 1H), 8.63 (dd, *J* = 8.0, 1.0 Hz, 1H), 8.60 (dd, *J* = 8.0, 1.0 Hz, 1H), 8.16 (dd, *J* = 8.0, 7.5 Hz, 1H), 7.83 (td, *J* = 8.1, 1.0 Hz, 1H), 7.68 (td, *J* = 8.1, 1.0 Hz, 1H), 7.41–7.53 (m, 8H), 7.24–7.31 (m, 2H). MS (EI+): *m/z* 427.1 (M⁺). Anal. Calcd for C₂₈H₁₇N₃O₂: C, 78.68; H, 4.01; N, 9.83. Found: C, 78.67; H, 4.09; N, 9.82.

1,2-Bis(hydroxydiphenylmethyl)indolizino[3,4,5-*ab*]isoindole (14). Indolizino[3,4,5-*ab*]isoindole-1,2-dicarboxylic acid dimethyl ester (**2**; 100 mg, 0.326 mmol) was dissolved in dry THF (20 mL). A 1.8 M phenyllithium solution in cyclohexane (0.80 mL, 1.43 mmol) was added dropwise at –75 °C under N₂ and stirred for 4 h, whereupon the solution turned yellow. The mixture was diluted with Et₂O (100 mL), washed with aqueous NH₄Cl (40 mL), then H₂O (40 mL), and dried over Na₂SO₄. The solvent was evaporated, and the residue was chromatographed on alumina with hexane/ethyl acetate = 1:1. Recrystallization from CH₂Cl₂/hexane afforded a yellow solid (110 mg, 0.198 mmol) in 61% yield. mp 284 °C (decomp). ¹H NMR (CD₂Cl₂): δ 8.33 (d, *J* = 7.5 Hz, 1H), 7.97 (d, *J* = 7.3 Hz, 1H), 7.15–7.40 (m, 24H), 7.14 (dd, *J* = 7.2, 1.0 Hz, 1H), 6.01 (t, *J* = 8.4 Hz), 6.00 (t, *J* = 8.4 Hz), 5.60 (s, 1H), 3.93 (s, 1H). MS (EI+): *m/z* 555.2 (M⁺), 538.2 (M⁺ – OH). Anal. Calcd for C₄₀H₂₉NO₂: C, 86.46; H, 5.26; N, 2.52. Found: C, 86.36; H, 5.22; N, 2.49. IR (DRIFT): ν (OH) 2800–3400 cm⁻¹.

1,1,3,3-Tetraphenyl-1,3-dihydrofuro[3',4':1,2]indolizino[3,4,5-*ab*]isoindole (15). 1,2-Bis(hydroxydiphenylmethyl)indolizino[3,4,5-*ab*]isoindole (**14**; 300 mg, 0.540 mmol) was dissolved in THF (100 mL) and acetic acid (10 mL) was added dropwise to this solution. The mixture was stirred at 80 °C for 4 h. The resulting mixture was diluted with CH₂Cl₂ (100 mL), washed with H₂O (2 × 50 mL), and dried over

Na₂SO₄. The solvent was evaporated, and the residue was chromatographed on alumina with CH₂Cl₂/hexane = 1:1. Recrystallization from CH₂Cl₂/hexane afforded a fine yellow solid (160 mg, 0.30 mmol) in 55% yield. mp 317 °C (decomp). *T*_g 300 °C.⁴² ¹H NMR (CD₂Cl₂): δ 8.48 (d, *J* = 8.0 Hz, 1H), 8.20 (d, *J* = 7.3 Hz, 1H), 8.06 (d, *J* = 8.3 Hz, 1H), 7.99 (d, *J* = 8.1 Hz), 7.77 (dd, *J* = 8.3, 7.3 Hz), 7.67 (t, *J* = 8.1 Hz, 1H), 7.45–7.55 (m, 9H), 7.16–7.26 (m, 12H). MS (EI+): *m/z* 537.2 (M⁺). Anal. Calcd for C₄₀H₂₇NO: C, 89.36; H, 5.06; N, 2.61. Found: C, 89.00; H, 5.45; N, 2.49.

Cyclic Voltammetry Measurement. Cyclic voltammetry (CV) was performed with a three-electrode cell in an acetonitrile solution of 0.1 M tetrabutylammonium hexafluorophosphate (Bu₄NPF₆) at a scan rate of 100 mV/s. A Pt wire was used as a counter electrode, and glassy carbon was used as working electrode and a Ag/AgNO₃ (0.1 M) electrode was used as a reference electrode. Its potential was corrected to the saturated calomel electrode (SCE) by measuring the ferrocene/ferrocenium couple in this system (0.44 V versus SCE).⁴³

Computational Methods. The GAUSSIAN 98⁴⁴ series of programs was used for all calculations. All molecules were fully optimized using the hybrid density functional⁴⁵ B3LYP level⁴⁶ of theory with the 6-31G(d) basis set. All optimized structures were found to be planar by frequency analysis. Proton affinities were evaluated at B3LYP/6-311+G(2d,p) level corrected for unscaled zero point vibrational energies (ZPVE) at B3LYP/6-31G(d) level using the B3LYP/6-31G(d) optimized geometries. Vertical ionization potential was calculated at B3LYP/6-311+G(2d,p) level using the B3LYP/6-31G(d) optimized geometry. Reorganization energy was calculated as an energy difference between cation radical, keeping geometry frozen to neutral molecule, and relaxed cation radical. Orbitals and normalized squares of the orbital coefficients (C²) were calculated at MP2/6-31G(d) density using B3LYP/6-31G(d) geometries.

X-ray Crystal Structure. Diffraction data were collected at low temperature (100 K) with graphite-monochromatized Mo Kα radiation (λ = 0.710 73 Å). The cell parameters were obtained from the least-squares refinement of the spots using the SMART program. The structure was solved by direct method using SHELXS-97, which revealed the positions of all non-hydrogen atoms. This was followed by several cycles of full-matrix least-squares refinement. Absorption corrections were applied by using SADABS.⁴⁷ Hydrogen atoms were included as fixed contributors to the final refinement cycles. The positions of hydrogen atoms were calculated on the basis of idealized geometry. In the final refinement, all non-hydrogen atoms were refined with anisotropic thermal coefficients.

Fabrication of Light-Emitting Devices. The ITO layer on glass substrate was 120 nm thick with a sheet resistance of about 20 Ω/. The stripe pattern with 2 mm wide of the ITO layer was etched by means of conventional photolithographic technique. Prior to the organic

- (42) This glass transition temperature is considerably high, which means this compound could have high thermal stability in a device. The ball-shape structure could be a good methodology for high *T*_g compounds.
- (43) Clerac, R.; Cotton, F. A.; Dunbar, K. R.; Lu, T.; Murillo, C. A.; Wang, X. *J. Am. Chem. Soc.* **2000**, *122*, 2272.
- (44) Frisch, M. J.; Trucks, G. W.; Schlegel, H. B.; Scuseria, G. E.; Robb, M. A.; Cheeseman, J. R.; Zakrzewski, V. G.; Montgomery, J. A., Jr.; Stratmann, R. E.; Burant, J. C.; Dapprich, S.; Millam, J. M.; Daniels, A. D.; Kudin, K. N.; Strain, M. C.; Farkas, O.; Tomasi, J.; Barone, V.; Cossi, M.; Cammi, R.; Mennucci, B.; Pomelli, C.; Adamo, C.; Clifford, S.; Ochterski, J.; Petersson, G. A.; Ayala, P. Y.; Cui, Q.; Morokuma, K.; Rega, N.; Salvador, P.; Dannenberg, J. J.; Malick, D. K.; Rabuck, A. D.; Raghavachari, K.; Foresman, J. B.; Cioslowski, J.; Ortiz, J. V.; Baboul, A. G.; Stefanov, B. B.; Liu, G.; Liashenko, A.; Piskorz, P.; Komaromi, I.; Gomperts, R.; Martin, R. L.; Fox, D. J.; Keith, T.; Al-Laham, M. A.; Peng, C. Y.; Nanayakkara, A.; Challacombe, M.; Gill, P. M. W.; Johnson, B.; Chen, W.; Wong, M. W.; Andres, J. L.; Gonzalez, C.; Head-Gordon, M.; Replogle, E. S.; Pople, J. A. *Gaussian 98*, Revision A.11.4; Gaussian, Inc.: Pittsburgh, PA, 2002.
- (45) (a) Parr, R. G.; Yang, W. *Density-Functional Theory of Atoms and Molecules*; Oxford University Press: New York, 1989. (b) Koch, W.; Holthausen, M. C. *A Chemist's Guide to Density Functional Theory*; Wiley-VCH: Weinheim, Germany, 2000.
- (46) (a) Lee, C.; Yang, W.; Parr, R. G. *Phys. Rev. B* **1988**, *37*, 785. (b) Becke, A. D. *J. Chem. Phys.* **1993**, *98*, 5648.
- (47) Blessing, R. H. *Acta Crystallogr.* **1995**, *A51*, 33.

deposition, the patterned ITO glass was ultrasonically cleaned with detergent, rinsed in water, and finished with the UV-ozone method. The hole-blocking material (SAIq) was synthesized according to literature procedures⁴⁸ and sublimed twice prior to use. All the other materials were purified by sublimation method prior to use. Evaporation was carried out at a pressure of about 2×10^{-6} Torr. The deposition rate of each organic layer was typically 0.1–0.3 nm/s. After the deposition of the organic layers, the bilayer cathode was successively deposited with a metal shadow mask, which defines a 2 mm stripe cathode pattern perpendicular to the ITO anode stripe. The thickness of the MgF₂ insulating layer was 1.5 nm, capped with an aluminum layer of 80 nm.

The luminance of the EL cell was measured with a luminance meter (Minolta LS-110) and the I–V characteristics were measured by an electrometer (HP 4140B). These measurements were all carried out in an ambient atmosphere. The electroluminescence spectra of the devices were measured by a multichannel photodiode array system (Otsuka Electronics MCPD-2000).

(48) Moore, C. P.; Slyke, V.; Arland, S.; Gysling, H. J. Eur. Pat. Appl. No. 579151, 1996.

Acknowledgment. We are grateful to Dr. S. I. Khan for X-ray crystallographic analysis (Department of Chemistry and Biochemistry, UCLA). We are grateful to Mitsubishi Chemical Corp. for support of T.M.

Supporting Information Available: General experimental procedure, crystal data, atomic coordinates, bond length, bond angles, anisotropic displacement parameters, hydrogen coordinates, isotropic displacement parameters, and torsion angles for compounds **2**, **6**, and **7**, absorption and fluorescence spectra of all **INIs** synthesized as well as λ_{max} of absorption spectra, λ_{max} of fluorescence spectra, and the Stokes shift, and absolute energies and optimized geometries (in Cartesian coordinates) for all calculated compounds at B3LYP/6-31G(d) (PDF, CIF). This material is available free of charge via the Internet at <http://pubs.acs.org>.

JA049214X